

A Generalization Bound for a Family of Implicit Networks

Samy Wu Fung

Department of Applied Mathematics and Statistics
Colorado School of Mines

Benjamin Berkels

Department of Mathematics
RWTH Aachen University

Abstract

Implicit networks are a class of neural networks whose outputs are defined by the fixed point of a parameterized operator. They have enjoyed success in many applications including natural language processing, image processing, and numerous other applications. While they have found abundant empirical success, theoretical work on its generalization is still under-explored. In this work, we consider a large family of implicit networks defined parameterized contractive fixed point operators. We show a generalization bound for this class based on a covering number argument for the Rademacher complexity of these architectures.

1 Introduction

Implicit networks El Ghaoui et al. (2021) are a class of neural network architectures whose outputs are defined by the fixed point of a parameterized operator $T_\psi(x, d)$. Mathematically, given inputs $d \in \mathbb{R}^m$ and network parameters $\theta = (\phi, \psi) \in \mathbb{R}^p$, an implicit network outputs a fixed point $x_{\psi, d}^*$, or often applies one additional layer to the fixed point, i.e., it outputs $P_\phi(x_{\psi, d}^*)$, where

$$x_{\psi, d}^* = T_\psi(x_{\psi, d}^*; d). \quad (1)$$

These networks are also known as deep equilibrium networks Bai et al. (2019) and in some settings, differentiable optimization layers Amos and Kolter (2017), and have been found to be effective for different tasks including natural language processing Bai et al. (2019), image processing Heaton and Wu Fung (2023); Zhao et al. (2023); Gilton et al. (2021), classification Wu Fung et al. (2022), traffic flow McKenzie et al. (2024a), control Gelphman et al. (2025), shortest path and knapsack problems McKenzie et al. (2024b), and more. The success of implicit networks is owed to their unique ability to incorporate hard constraints directly

into the output representation Heaton and Wu Fung (2023); Heaton et al. (2021), enabling precise control over the properties of the learned functions. This flexibility allows for the enforcement of geometric, physical, or structural constraints that are often difficult to impose in traditional neural network architectures. Additionally, implicit networks have empirically been found to extrapolate; that is, they can be trained on easy tasks (e.g., solving small 9×9 mazes) and solving larger mazes Anil et al. (2022); Knutson et al. (2024). These strengths make implicit networks a powerful tool for applications where both adherence to specific constraints and robust extrapolation are crucial.

While many generalization works exist for deep neural networks Bartlett et al. (2017); Golowich et al. (2018), and continuous time networks Marion (2024), to our knowledge, only two prior works exist for implicit networks, one based on Monotone Equilibrium Networks Pabbbaraju et al. (2020) which relies on the monotonicity properties to establish bounds, and another which examines over-parameterized implicit networks Gao and Gao (2022). This work extends these efforts by presenting a generalization bound applicable to a broader class of implicit networks, encompassing various architectures beyond those previously studied.

1.1 Our Contribution

In this work, we prove a generalization bound for a large family of implicit networks defined by a contractive fixed point operator. These encompass implicit architectures such as Monotone Equilibrium Networks Winston and Kolter (2020), single-layer implicit networks El Ghaoui et al. (2021), and optimization-based implicit networks Heaton and Wu Fung (2023); Yin et al. (2022). The core idea is to use a covering number argument based on Dudley's inequality to bound the Rademacher complexity.

2 Related Work

Continuous-Time Neural Networks. To our knowledge, the first generalization bound for

Table 1: Nomenclature

m : input dimension	n : output dimension
$p = p_\Phi + p_\Psi$: number of parameters	N : number of samples
$d \in \mathbb{R}^m$: input data	$y \in \mathbb{R}^n$: output data
$\mathcal{Y} \subset \mathbb{R}^n$: compact set for variables y	$\mathcal{D} \subset \mathbb{R}^m$: compact set for variables d
$\ell: \mathbb{R}^n \times \mathbb{R}^n \rightarrow \mathbb{R}$: loss function	$\theta = (\phi, \psi) \in \mathbb{R}^p$ network parameters
$\mathcal{L}(\theta)$: expected loss	$\hat{\mathcal{L}}(\theta)$: empirical loss
$S = \{(d_i, y_i)\}_{i=1}^N$: sample set	$D = [d_1, d_2, \dots, d_N] \in \mathbb{R}^{m \times N}$: stacked inputs
C_{params} : bound on norm of network parameters	C_{out} : bound on output of neural network
C_ℓ : bound on loss ℓ	$T_\psi(x; d)$: fixed point operator
L_x : Lipschitz constant of T w.r.t x	L_ψ : Lipschitz constant of T w.r.t ψ
L : Lipschitz constant of fixed point mapping	C_d bound on norm of variables $d \in \mathcal{D}$
k : dimension of x , i.e. $x_{\psi, d}^* \in \mathbb{R}^k$	$P_\phi: \mathbb{R}^k \rightarrow \mathbb{R}^n$ final layer
$\Theta = \Phi \times \Psi \subset \mathbb{R}^p$: admissible parameters	$B_r(x) := B_r^X(x) := \{y \in X : \ x - y\ _X < r\}$

continuous-time neural networks (i.e., neural ODEs Chen et al. (2018)) is provided in Marion (2024), where boundedness and Lipschitz assumptions on the parameters of the neural ODE and Lipschitz continuous loss functions are required. Bleistein and Guilloux (2024) extend this work for neural controlled differential equations (NCDEs) which use a Lipschitz-based argument to obtain a sampling-dependent generalization bound for NCDEs.

Recurrent and Unrolled Neural Networks. Zhang et al. (2018) use a PAC-Bayes approach based on the empirical Rademacher complexity to establish a generalization bound for vanilla RNNs. This work is extended by Chen et al. (2020), which presents a tighter bound by incorporating the boundedness condition of the hidden state into their analysis. A special class of RNNs, called unrolled networks Gregor and LeCun (2010); Adler and Öktem (2018) unroll an optimization algorithm to perform inferences. Behboodi et al. (2022) provide a generalization bound for this class of networks in the context of compressive sensing. This work is based on bounding the Rademacher complexity and provides a bound that grows logarithmically in the number of layers.

Implicit Networks. Our work is most closely related to Pabbaraju et al. (2020), which provides generalization bounds for a specific class of implicit networks, known as monotone operator deep equilibrium networks (MON-DEQs) Winston and Kolter (2020). In this work, a generalization bound that is also based on bounding the Rademacher complexity is provided for MON-DEQs (see (Pabbaraju et al., 2020, Theorem 3)) following techniques from Neyshabur et al. (2017). Rather than focus on MONs, our work provides a bound for arbitrary contractive operators T_ψ . Another key difference is that our work provides a bound for the standard empirical loss instead of the empirical margin loss Pabbaraju et al. (2020). A more recent work

proves generalization bounds for fully trained over-parameterized implicit network Gao and Gao (2022), adapting NTK-based analysis to implicit models. Although our bound applies to a broader family of architectures, the complexity of the bounds makes it less clear how their tightness compares.

3 Preliminaries

Consider the supervised learning setting with a sample set of input-output pairs $S = \{(d_i, y_i)\}_{i=1}^N$ sampled from unknown distribution \mathbb{P}_{true} . We define the expected and empirical loss by

$$\begin{aligned} \mathcal{L}(\theta) &= \mathbb{E}_{(d, y) \sim \mathbb{P}_{\text{true}}} [\ell(P_\phi(x_{\psi, d}^*), y)] \quad \text{and} \\ \hat{\mathcal{L}}(\theta) &= \frac{1}{N} \sum_{i=1}^N \ell(P_\phi(x_{\psi, d_i}^*), y_i), \end{aligned} \quad (2)$$

respectively, where $x_{\psi, d}^*$ is a fixed point defined in (1), $\ell: \mathbb{R}^n \times \mathbb{R}^n \rightarrow \mathbb{R}$ is a discrepancy function and \mathbb{P}_{true} is the joint distribution of input-output pairs. For any parameter θ , the generalization bound we prove in this work will provide an upper bound for $|\mathcal{L}(\theta) - \hat{\mathcal{L}}(\theta)|$. For ease of presentation, we provide a table for the variable nomenclature that will be used throughout this paper in Table 1. Additionally, $\|\cdot\|$ is taken to be the Euclidean norm henceforth (unless stated otherwise) for brevity.

We denote the set of all hypothesis functions by

$$\begin{aligned} \mathcal{H} &= \left\{ h: \mathbb{R}^m \rightarrow \mathbb{R}^n : \exists \theta = (\phi, \psi) \in \Theta \ \forall d \in \mathbb{R}^m \right. \\ &\quad \left. h(d) = P_\phi(x_{\psi, d}^*) \right\}. \end{aligned} \quad (3)$$

Moreover, let $D = [d_1, d_2, \dots, d_N] \in \mathbb{R}^{m \times N}$ be the concatenated set inputs from the sample set S , and define the set of all possible concatenated outputs as

$$\mathcal{M} = \{P_\phi(x_{\psi, d}^*) \in \mathbb{R}^{n \times N} : \theta = (\phi, \psi) \in \Theta\}. \quad (4)$$

Definition 1. An operator $F: \mathbb{R}^n \rightarrow \mathbb{R}^n$ is contractive with parameter $\kappa \in (0, 1)$ if

$$\|F(x) - F(y)\| \leq \kappa \|x - y\| \quad \forall x, y \in \mathbb{R}^n. \quad (5)$$

Definition 2 (Talagrand (2021), Definition 1.4.1). Let (\mathcal{M}, d) be a metric space and $r > 0$. Then the covering number $\mathcal{N}(\mathcal{M}, d, r)$ of (\mathcal{M}, d) at level r is the smallest $n \in \mathbb{N}$ such that \mathcal{M} can be covered by n balls of radius r .

Remark 1. When the metric is induced by a norm, we write $\mathcal{N}(\mathcal{M}, \|\cdot\|, r)$.

Definition 3 (Empirical Rademacher Complexity). Consider a class of scalar, real-valued functions \mathcal{G} and a sample set $Z = (z_1, z_2, \dots, z_N)$. Then, the empirical Rademacher complexity is defined as

$$R_Z(\mathcal{G}) = \mathbb{E}_\epsilon \sup_{g \in \mathcal{G}} \frac{1}{N} \sum_{i=1}^N \epsilon_i g(z_i) \quad (6)$$

where $\epsilon \in \mathbb{R}^N$ is a Rademacher vector, i.e., a vector of independent Rademacher variables $\epsilon_i, i = 1, \dots, N$ taking the values ± 1 with equal probability.

Remark 2. Note the Rademacher complexity is with respect to an entire class of functions \mathcal{G} in the definition above.

Definition 4 (Subgaussian Process, Foucart and Rauhut (2013), Definition 8.22). Consider a stochastic process $(Z_t)_{t \in \mathcal{T}}$ with the index set \mathcal{T} in a space with pseudometric given by

$$d(s, t) = (\mathbb{E}|Z_s - Z_t|^2)^{1/2}. \quad (7)$$

Let $(Z_t)_{t \in \mathcal{T}}$ be centered, i.e., $\mathbb{E}Z_t = 0$ for all $t \in \mathcal{T}$. Then, $(Z_t)_{t \in \mathcal{T}}$ is called subgaussian if

$$\mathbb{E} \exp(\omega(Z_s - Z_t)) \leq \exp\left(\frac{\omega^2 d(s, t)^2}{2}\right) \quad (8)$$

$$\forall s, t \in \mathcal{T}, \omega > 0.$$

Moreover, the radius of such a process is defined by

$$\Delta(\mathcal{T}) = \sup_{t \in \mathcal{T}} \sqrt{\mathbb{E}|Z_t|^2}. \quad (9)$$

Remark 3. In this work, \mathcal{T} will correspond to all possible hypothesis functions generated by a neural network architecture, and Z_t will correspond to the loss evaluated at a particular choice of parameters for a fixed training set.

The next two results are the key tools we use to show our generalization bounds.

Theorem 1 (Dudley's Inequality, Theorem 8.23 Foucart and Rauhut (2013)). Let $(Z_t)_{t \in \mathcal{T}}$ be a centered subgaussian process with radius $\Delta(\mathcal{T})$. Then

$$\mathbb{E} \sup_{t \in \mathcal{T}} Z_t \leq 4\sqrt{2} \int_0^{\Delta(\mathcal{T})/2} \sqrt{\log(\mathcal{N}(\mathcal{T}, d, r))} dr \quad (10)$$

Theorem 2 (Theorem 26.5, Shalev-Shwartz and Ben-David (2014)). Let \mathcal{H} be a family of functions, \mathcal{S} be the training set of N input-output pairs drawn from \mathbb{P}_{true} and ℓ be a real-valued bounded loss function satisfying $|\ell(h(d), y)| \leq C_\ell$ for all $h \in \mathcal{H}$ and data pairs $(d, y) \in \mathbb{R}^m \times \mathbb{R}^n$. Then with probability at least $1 - \delta$ we have, for all $h \in \mathcal{H}$,

$$\mathcal{L}(h) \leq \hat{\mathcal{L}}(h) + 2\mathcal{R}_S(\ell \circ \mathcal{H}) + 4C_\ell \sqrt{\frac{2 \log(4/\delta)}{N}}, \quad (11)$$

where $\ell \circ \mathcal{H}$ is to be understood as

$$\ell \circ \mathcal{H} = \{\mathbb{R}^m \times \mathbb{R}^n \rightarrow \mathbb{R}, (d, y) \mapsto \ell(h(d), y) : h \in \mathcal{H}\}. \quad (12)$$

Remark 4. Dudley's inequality will allow us to bound the Rademacher complexity using a covering number argument.

4 Generalization of Implicit Networks

We state a series of assumptions and lemmas necessary for our result. For ease of presentation, all proofs are provided in the appendix.

Assumption 1. The distribution of the training data \mathbb{P}_{true} has compact support. We denote these sets by $\mathcal{D} \times \mathcal{Y}$ with $\mathcal{D} \subset \mathbb{R}^m, \mathcal{Y} \subset \mathbb{R}^n$.

Assumption 2. The loss function $\ell: \mathbb{R}^n \times \mathbb{R}^n \rightarrow \mathbb{R}$ is Lipschitz with constant L_ℓ .

Assumption 3 (Bounded Network Parameters and Fixed Points). The set of parameters and fixed points are bounded. That is,

$$\begin{aligned} \theta &\in \Theta = \Phi \times \Psi \text{ where} \\ \Phi &= \{\phi \in \mathbb{R}^{p_\Phi} : \|\phi\| \leq C_{\text{params}, \Phi}\} \\ \text{and } \Psi &= \{\psi \in \mathbb{R}^{p_\Psi} : \|\psi\| \leq C_{\text{params}, \Psi}\} \\ \text{and } \|x_{\psi, d}^*\| &\leq C_{\text{out}, T} \\ \text{and } \|P_\phi(x_{\psi, d}^*)\| &\leq C_{\text{out}} \text{ for all } \theta = (\phi, \psi) \in \Theta, d \in \mathcal{D} \end{aligned} \quad (13)$$

for $C_{\text{params}, \Phi}, C_{\text{params}, \Psi}, C_{\text{out}, T}, C_{\text{out}} > 0$.

Assumption 4 (Lipschitz Properties of Fixed Point Operator). The operator $\Psi \times \mathbb{R}^n \times \mathcal{D} \rightarrow \mathbb{R}^n, (\psi, x, d) \mapsto T_\psi(x; d)$ is contractive in x with constant $L_x \in (0, 1)$. Moreover, define $\mathcal{X}^* = \{x_{\psi, d}^* : d \in \mathcal{D}, \psi \in \Psi\}$ to be the set of all possible fixed points. The operator $\Psi \times \mathcal{X}^* \times \mathcal{D} \rightarrow \mathbb{R}^n, (\psi, x, d) \mapsto T_\psi(x; d)$ is Lipschitz with respect to ψ whenever $x \in \mathcal{X}^*$ with constant L_ψ . The mapping $\Phi \times \overline{B_{C_{\text{out}, T}}^{\mathbb{R}^k}(0)} \rightarrow \mathbb{R}^n : (\phi, x) \mapsto P_\phi(x)$ is Lipschitz in ϕ with constant $L_{P, \phi}$ and Lipschitz in x with constant $L_{P, x}$. Here, $B_r^X(x) := \{y \in X : \|x - y\|_X < r\}$ is the ball with radius $r > 0$ centered at $x \in X$ for a normed vector space X .

We note these assumptions can often be enforced in practice. For example, contractivity of $T_\psi(x; d)$ with respect to x can be obtained using, e.g., spectral normalization Miyato et al. (2018). Moreover, one may enforce the output of the network, $x_{\psi, d}^*$, by composing it with a projection onto the ball of radius C_{out} .

Next, we state some results that must be proven in order to obtain our generalization bound. In particular, the core idea is to bound the Rademacher complexity and plug this bound into Theorem 2.

Lemma 1. *Under Assumption 4, the fixed point mapping $\Psi \times \mathcal{D} \rightarrow \mathbb{R}^n, (\psi, d) \mapsto x_{\psi, d}^*$ is Lipschitz with respect to θ with constant $L = \frac{L_\psi}{1 - L_x}$.*

Lemma 2. *Under Assumption 4, the mapping $\Theta \times \mathcal{D} \rightarrow \mathbb{R}^n, ((\phi, \psi), d) \mapsto P_\phi(x_{\psi, d}^*)$ is Lipschitz with respect to $\theta = (\phi, \psi)$ with constant $\hat{L} = \sqrt{(L_{P, x} L)^2 + L_{P, \phi}^2}$.*

Lemma 3 (Bound on Rademacher Complexity). *Under Assumptions 2, 3, and 4, we have*

$$\mathcal{R}_S(\ell \circ \mathcal{H}) \leq \frac{8L_\ell}{N} \int_0^{\sqrt{NC_{\text{out}}}/2} \sqrt{\log \mathcal{N}(\mathcal{M}, \|\cdot\|, r)} dr. \quad (14)$$

where L_ℓ is the Lipschitz constant of ℓ .

Lemma 4 (Bound on Covering Number). *Under Assumptions 4 and 3,*

$$\mathcal{N}(\mathcal{M}, \|\cdot\|, r) \leq \left(1 + \frac{2\hat{L}C_{\text{params}}}{r}\right)^p, \quad (15)$$

where $C_{\text{params}} = \sqrt{C_{\text{params}, \Phi}^2 + C_{\text{params}, \Psi}^2}$.

Lemma 5 (Bound on Loss Function). *Under Assumptions 1, 2, there exists a constant $C_\ell > 0$ such that*

$$|\ell(P_\phi(x_{\psi, d}^*), y)| \leq C_\ell \quad \forall (d, y) \sim \mathbb{P}_{\text{true}}, \forall \theta = (\phi, \psi) \in \Theta. \quad (16)$$

We now state our main result.

Theorem 3 (Generalization Bound). *Under Assumptions 1–4, for any $\theta \in \Theta$ and $\delta \in (0, 1)$, we have*

$$\begin{aligned} \mathcal{L}(\theta) &\leq \hat{\mathcal{L}}(\theta) \\ &+ 8L_\ell C_{\text{out}} \sqrt{\frac{p}{N} \cdot \log \left(e \cdot \left(1 + \frac{4\hat{L}C_{\text{params}}}{\sqrt{NC_{\text{out}}}} \right) \right)} \\ &+ 4C_\ell \sqrt{\frac{2 \log(4/\delta)}{N}} \end{aligned} \quad (17)$$

with probability $1 - \delta$.

A few remarks are in order. First, we follow the generalization bound proof technique from Behboodi et al. (2022); however, the resulting bound *does not* depend on the “depth” of the network as in Behboodi et al. (2022). The generalization error is upper bounded by a noise induced term and a complexity term which grows with the square root of the model’s complexity measured by the number of parameters p . Similar to most related works stated in Section 2, this uses a Lipschitz-based argument and the result is obtained by upper-bounding the Rademacher complexity. Our proof assumes Lipschitzness of the operator T_ψ as well as boundedness and a Lipschitz condition on the loss function ℓ . We also note that the log term approaches 1 as $N \rightarrow \infty$, thus, the bound is $\mathcal{O}(1/\sqrt{N})$. Finally, the generalization bound in Theorem 3 relies boundedness of the network parameters and outputs. This assumption should be understood as a theoretical condition on the admissible hypothesis class rather than a claim about the implicit behavior of unconstrained optimization algorithms. But we emphasize that the admissible parameter radius need not be small. The theoretical results hold for *any* finite bound, and in practice the radius can be chosen sufficiently large so that the constraint is effectively inactive over the course of training. In this sense, boundedness serves as a technical device required for the covering-number argument rather than a restrictive modeling assumption.

5 Example Architectures

We prove Lipschitzness of some standard implicit architectures. Since the set of training data has compact support, we denote the maximum norm of samples d to be C_d . That is, $\|d\| \leq C_d$ for all d in \mathcal{D} .

If $k = n$, i.e., the output of the fixed point iteration has the same dimension as the output data, the layer P_ϕ is usually not necessary, so it can be chosen as the identity, i.e., $P_\phi(x) = x$. In this case, we get $\Phi = \emptyset$, $p_\Phi = 0$, $C_{\text{params}, \Phi} = 0$, $L_{P, x} = 1$, $L_{P, \phi} = 0$ and thus $\hat{L} = \sqrt{((1 \cdot L)^2 + 0^2)} = L$.

If $k \neq n$, P_ϕ is needed to convert the dimension of the fixed point to the one of the output data. Here, it is often sufficient to choose P_ϕ as a linear layer, i.e., $\phi = A \in \mathbb{R}^{n \times k}$ and $P_A(x) = Ax$. In this case, $L_{P, x} = C_{\text{params}, \Phi}$ and $L_{P, \phi} = C_{\text{out}, T}$.

5.1 Single-Layer Contractive Implicit Network

Perhaps the most standard architecture is a contractive implicit network with fixed point operator of the form

$$T_\psi(x; d) = \sigma(Wx + Ud + b), \quad (18)$$

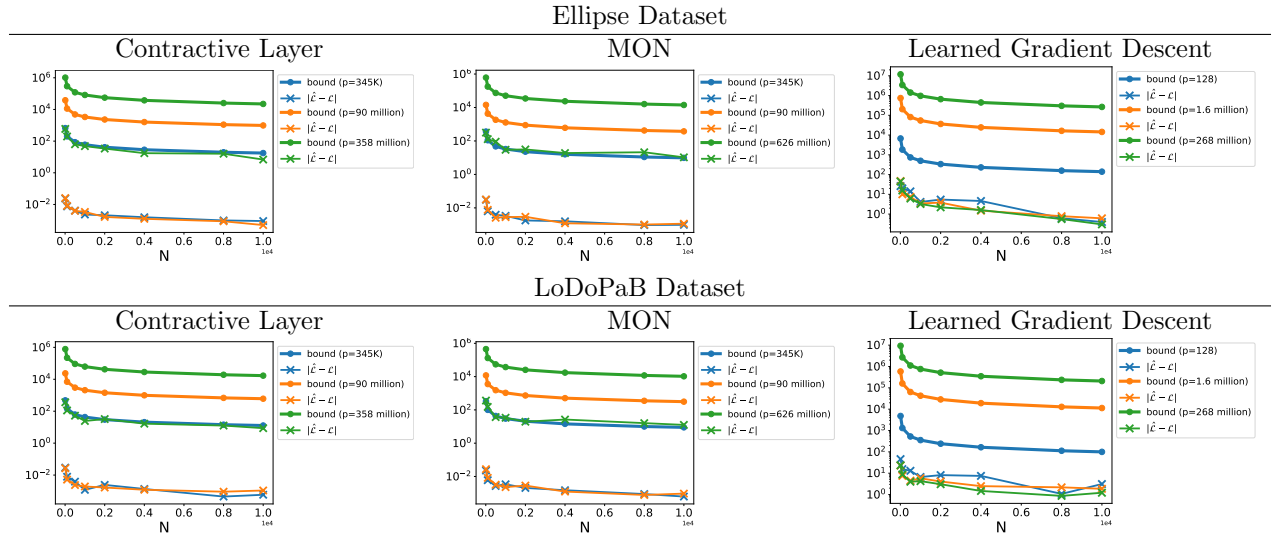


Figure 1: Generalization bound (and errors) for different implicit architectures and for different number of parameters p . On the x-axis, we have the number of samples (note these are multiplied by 10^4).

where contractivity w.r.t. x can be guaranteed by using, e.g., spectral normalization Miyato et al. (2018) so that $\|W\| < 1$ and $\sigma: \mathbb{R} \rightarrow \mathbb{R}$ is a 1-Lipschitz non-linear activation function, e.g., ReLU. Here, the parameters to be learned are $\psi = (W, U, b)$.

Lemma 6 (Lipschitz Property of Contractive Networks). *Let T_ψ be given by (18). Under Assumption 3, T_ψ satisfies Assumption 4 with $L_x = \|W\|$ and $L_\psi = \sqrt{C_{out}^2 + C_d^2 + 1}$.*

5.2 Monotone Equilibrium Network

We begin with a MON architecture given by the forward-backward iteration described in Section 2 Pabbaraju et al. (2020):

$$T_\psi(x; d) = \sigma((I - \alpha(I - W))x + \alpha(Ud + b)), \quad (19)$$

where $\sigma: \mathbb{R} \rightarrow \mathbb{R}$ is a 1-Lipschitz non-linearity. To ensure T is contractive, one must ensure $I - W$ is strongly monotone; this is achieved by parameterizing $W = (1 - m)I - A^\top A + B - B^\top$ for some matrices A, B , and $0 \leq \alpha \leq 2m/\|I - W\|^2$ where m is the strong monotonicity parameter. Here, the parameters to be learned are $\psi = (A, B, U, b)$.

Lemma 7 (Lipschitz Property of MONs). *Let T_ψ be given by (19). Under Assumption 3, T_ψ satisfies Assumption 4 with $L_\psi = \alpha\sqrt{4(C_{params}^2 + 1)C_{out}^2 + C_d^2 + 1}$ and $L_x < 1$.*

5.3 Gradient-Descent Based Network

In inverse problems, it is of interest to learn a regularization operator R Alberti et al. (2021) arising from

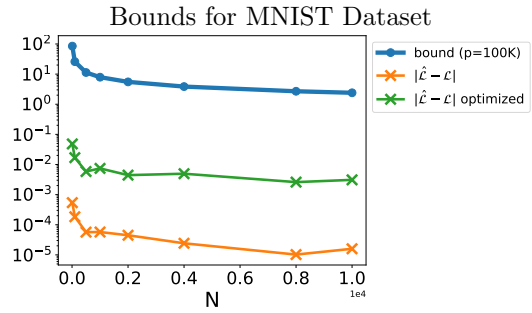


Figure 2: Generalization bound for the MNIST dataset. Here, the blue line represents the generalization bound, and the green and orange line represent the generalization error for an optimized and random set of weights, respectively

a problem of the form

$$\min_x \frac{1}{2} \|Ax - b\|^2 + \frac{1}{2} \|Rx\|^2 \quad (20)$$

In this case, one may learn a gradient descent scheme where the fixed point operator is given by

$$T_\psi(x; d) = x - \alpha(A^\top(Ax - d) + R^\top Rx) \quad (21)$$

Here, A is given and $\psi = R \in \mathbb{R}^{n_1 \times n}$ is the regularization operator to be learned and $\alpha \in (0, \frac{2}{\lambda_{\max}(A^\top A + R^\top R)})$ Ryu and Yin (2022).

Lemma 8 (Lipschitz Property of Learned Gradient Descent). *Let T_ψ be given by (21). Under Assumption 3, T_ψ satisfies Assumption 4 with $L_\psi = 2\alpha C_{out} C_{params, \Psi}$ and $L_x < 1$.*

6 Experiments

6.1 Data Setup

We use a set of different datasets to test our generalization bounds. The first dataset is the LoDoPaB dataset Leuschner et al. (2021); Heaton et al. (2022) and the MNIST dataset LeCun (1998). We choose the MNIST dataset because it is a standard benchmark for image classification tasks, which allows us to evaluate our framework using the cross-entropy loss composed with the softmax activation. Moreover, we choose the LoDoPaB dataset because it is widely adopted in *learning-to-optimize* studies, where the network architecture is designed to resemble an optimization algorithm such as our learned gradient descent model.

For the LoDoPaB data, CT measurements are simulated with a parallel beam geometry with a sparse-angle setup of only 30 angles and 183 projection beams, resulting in 5,490 equations and 16,384 unknowns. In these experiments, 1.5% Gaussian noise corresponding to each individual beam measurement is added to the measurements. The images have a resolution of 128×128 pixels. The ellipse training and test sets contain 11,000 total sample pairs. The LoDoPaB training and test sets contain 22,000 sample pairs, respectively.

6.2 Experimental Setup and Results

For all three architectures, we estimate the required constants; these include C_{out} , C_{params} , and C_d . To estimate C_{out} , we compute x_d^* for all d in the dataset over 100 randomly generated samples of θ . The constant L_x is not estimated but deliberately chosen to be 0.9 to ensure the network's contractivity. This is achieved through *spectral normalization* Miyato et al. (2018), which enforces a bound on the spectral norm of the weight matrices using the power iteration method Golub and Van Loan (2013).

To compute C_d , we find the maximum norm of each of the samples provided. To find C_{params} , we normalize each of the weights to have norm 1; specifically, we bound $\|A\|, \|B\|, \|U\|, \|b\| \leq 1$ so that $C_{\text{params}} = \sqrt{4}$ for MON. We also bound $\|W\|, \|U\|, \|b\| \leq 1$ so that $C_{\text{params}} \leq \sqrt{3}$ for the single layer contractive network, and $\|R\| \leq 1$ for the learned gradient descent network. For the CT dataset, we choose $P_\phi(x) = x$, and for the MNIST dataset, we choose a linear final mapping layer given by $P_\phi(x) = \phi x$, where $\phi \in \mathbb{R}^{n \times k}$. Finally, we choose the ReLU activation function for all architectures for the CT dataset and the leaky ReLU activation for the MNIST data, which are commonly used in their respective tasks. Note both of these are non-expansive.

Moreover, we choose the l_1 -norm for $\ell(\cdot, \cdot)$ and the cross-entropy function for the MNIST dataset, and estimate their maximum bound in a similar manner to C_{out} . We note these choices of ℓ have Lipschitz constant $L_\ell = 1$ for $\ell = \|\cdot\|_1$ and $L_\ell = 2$ for the cross entropy function composed with softmax (see Lemma 9) in the appendix. We set $\delta = 10^{-2}$ for all experiments.

Figure 1 shows the generalization bound over different sample sizes N and different number of parameters p . As expected, the bound decreases for smaller N and p . We also observe similar results for the MNIST dataset in Figure 2, where we show the bound (in blue), the generalization error of a randomly initialized network (orange), and the generalization error of an optimized implicit network. Here, the x axis represents the number of samples used to estimate both, the bound and the errors. As expected, all bounds and errors behave like $\mathcal{O}(1/\sqrt{N})$. Moreover, we observe that the bounds are not particularly tight; however, this is to be expected for bounds that are especially general such as the one presented in this work, which can be applied to a large family of implicit networks. We also include a robustness experiment in Appendix B.

Finally, we note that in Figure 2, the optimized weights lead to a larger generalization discrepancy; this is because for randomly initialized neural networks, the predicted probabilities are roughly uniform, leading to the same prediction regardless of batchsize.

7 Conclusion

In this work, we derive a generalization bound for contractive implicit neural networks. Our bound employs a covering number argument to bound the Rademacher complexity of these architectures. Our work relies on Lipschitz assumptions of the fixed point operator as well as boundedness of the fixed point outputs. We note that while we only consider the implicit network, one can extend our bounds when embedding these as a differentiable layer in a larger architecture Amos and Kolter (2017). Some recent work that may aid in the further study of generalization of implicit networks reveals connections between implicit networks and Gaussian processes (Gao et al., 2023) and global convergence of implicit networks (Gao et al., 2022). We focus on providing a foundational generalization bound for a broad class of implicit neural networks defined via contractive fixed-point operators. While comparative studies with depth-equivalent explicit (unrolled) networks are of interest, a principled comparison would require matched assumptions and corresponding explicit-network bounds and is therefore left for future work. Finally, while contractivity can be enforced through techniques such as spec-

tral normalization and has proven effective in many settings Heaton and Wu Fung (2023); McKenzie et al. (2024a), such enforcement can potentially limit the expressive capacity of these networks. This trade-off helps explain why many successful implementations of implicit networks do not enforce strict global contractivity during training in practice. Instead, they rely on alternative stability mechanisms such as careful initialization and Jacobian regularization. Understanding how these stability mechanisms can play a role for a better generalization bound remains an important direction for future work.

Acknowledgments

Part of this research was performed while the authors were visiting the Institute for Pure and Applied Mathematics (IPAM), which is supported by the National Science Foundation, award number DMS-1925919. Samy Wu Fung was also partially funded by the National Science Foundation, award number DMS-2309810. Benjamin Berkels was supported by the German research foundation (DFG) within the Collaborative Research Centre SFB 1481 “Sparsity and Singular Structures” (Project ID 442047500, Project A08).

References

Adler, J. and Öktem, O. (2018). Learned primal-dual reconstruction. *IEEE transactions on medical imaging*, 37(6):1322–1332.

Alberti, G. S., De Vito, E., Lassas, M., Ratti, L., and Santacesaria, M. (2021). Learning the optimal tikhonov regularizer for inverse problems. *Advances in Neural Information Processing Systems*, 34:25205–25216.

Amos, B. and Kolter, J. Z. (2017). Optnet: Differentiable optimization as a layer in neural networks. In *International conference on machine learning*, pages 136–145. PMLR.

Anil, C., Pokle, A., Liang, K., Treutlein, J., Wu, Y., Bai, S., Kolter, J. Z., and Grosse, R. B. (2022). Path independent equilibrium models can better exploit test-time computation. *Advances in Neural Information Processing Systems*, 35:7796–7809.

Bai, S., Kolter, J. Z., and Koltun, V. (2019). Deep equilibrium models. *Advances in neural information processing systems*, 32.

Bartlett, P. L., Foster, D. J., and Telgarsky, M. J. (2017). Spectrally-normalized margin bounds for neural networks. *Advances in neural information processing systems*, 30.

Behboodi, A., Rauhut, H., and Schnoor, E. (2022). Compressive sensing and neural networks from a statistical learning perspective. In *Compressed Sensing in Information Processing*, pages 247–277. Springer.

Bleistein, L. and Guilloux, A. (2024). On the generalization and approximation capacities of neural controlled differential equations. In *The Twelfth International Conference on Learning Representations*.

Chen, M., Li, X., and Zhao, T. (2020). On generalization bounds of a family of recurrent neural networks. In *International Conference on Artificial Intelligence and Statistics*, pages 1233–1243. PMLR.

Chen, R. T., Rubanova, Y., Bettencourt, J., and Duvenaud, D. K. (2018). Neural ordinary differential equations. *Advances in neural information processing systems*, 31.

El Ghaoui, L., Gu, F., Travacca, B., Askari, A., and Tsai, A. (2021). Implicit deep learning. *SIAM Journal on Mathematics of Data Science*, 3(3):930–958.

Foucart, S. and Rauhut, H. (2013). *A Mathematical Introduction to Compressive Sensing*. Applied and Numerical Harmonic Analysis. Springer New York, New York, NY.

Gao, T. and Gao, H. (2022). On the optimization and generalization of overparameterized implicit neural networks. *arXiv preprint arXiv:2209.15562*.

Gao, T., Huo, X., Liu, H., and Gao, H. (2023). Wide neural networks as gaussian processes: Lessons from deep equilibrium models. *Advances in Neural Information Processing Systems*, 36:54918–54951.

Gao, T., Liu, H., Liu, J., Rajan, H., and Gao, H. (2022). A global convergence theory for deep reLU implicit networks via over-parameterization. In *International Conference on Learning Representations*.

Gelphman, E., Verma, D., Yang, N. T., Osher, S., and Fung, S. W. (2025). End-to-end training of high-dimensional optimal control with implicit hamiltonians via jacobian-free backpropagation. *arXiv preprint arXiv:2510.00359*.

Gilton, D., Ongie, G., and Willett, R. (2021). Deep equilibrium architectures for inverse problems in imaging. *IEEE Transactions on Computational Imaging*, 7:1123–1133.

Golowich, N., Rakhlin, A., and Shamir, O. (2018). Size-independent sample complexity of neural networks. In *Conference On Learning Theory*, pages 297–299. PMLR.

Golub, G. H. and Van Loan, C. F. (2013). *Matrix computations*. JHU press.

Gregor, K. and LeCun, Y. (2010). Learning fast approximations of sparse coding. In *Proceedings of the*

27th international conference on international conference on machine learning, pages 399–406.

Heaton, H. and Wu Fung, S. (2023). Explainable ai via learning to optimize. *Scientific Reports*, 13(1):10103.

Heaton, H., Wu Fung, S., Gibali, A., and Yin, W. (2021). Feasibility-based fixed point networks. *Fixed Point Theory and Algorithms for Sciences and Engineering*, 2021:1–19.

Heaton, H., Wu Fung, S., Lin, A. T., Osher, S., and Yin, W. (2022). Wasserstein-based projections with applications to inverse problems. *SIAM Journal on Mathematics of Data Science*, 4(2):581–603.

Knutson, B., Rabeendran, A. C., Ivanitskiy, M., Pettyjohn, J., Diniz-Behn, C., Wu Fung, S., and McKenzie, D. (2024). On logical extrapolation for mazes with recurrent and implicit networks. *arXiv preprint arXiv:2410.03020*.

LeCun, Y. (1998). The mnist database of handwritten digits. <http://yann.lecun.com/exdb/mnist/>.

Leuschner, J., Schmidt, M., Baguer, D. O., and Maass, P. (2021). LoDoPaB-CT, a benchmark dataset for low-dose computed tomography reconstruction. *Scientific Data*, 8(1):109.

Marion, P. (2024). Generalization bounds for neural ordinary differential equations and deep residual networks. *Advances in Neural Information Processing Systems*, 36.

Maurer, A. (2016). A vector-contraction inequality for rademacher complexities. In *Algorithmic Learning Theory: 27th International Conference, ALT 2016, Bari, Italy, October 19-21, 2016, Proceedings* 27, pages 3–17. Springer.

McKenzie, D., Heaton, H., Li, Q., Wu Fung, S., Osher, S., and Yin, W. (2024a). Three-operator splitting for learning to predict equilibria in convex games. *SIAM Journal on Mathematics of Data Science*, 6(3):627–648.

McKenzie, D., Wu Fung, S., and Heaton, H. (2024b). Differentiating through integer linear programs with quadratic regularization and davis-yin splitting. *Transactions on Machine Learning Research*.

Miyato, T., Kataoka, T., Koyama, M., and Yoshida, Y. (2018). Spectral normalization for generative adversarial networks. In *International Conference on Learning Representations*.

Neyshabur, B., Bhojanapalli, S., and Srebro, N. (2017). A pac-bayesian approach to spectrally-normalized margin bounds for neural networks. *arXiv preprint arXiv:1707.09564*.

Pabbaraju, C., Winston, E., and Kolter, J. Z. (2020). Estimating lipschitz constants of monotone deep equilibrium models. In *International Conference on Learning Representations*.

Ryu, E. K. and Yin, W. (2022). *Large-scale convex optimization: algorithms & analyses via monotone operators*. Cambridge University Press.

Shalev-Shwartz, S. and Ben-David, S. (2014). *Understanding machine learning: From theory to algorithms*. Cambridge university press.

Talagrand, M. (2021). *Upper and Lower Bounds for Stochastic Processes*. Springer, 2nd edition.

Winston, E. and Kolter, J. Z. (2020). Monotone operator equilibrium networks. *Advances in neural information processing systems*, 33:10718–10728.

Wu Fung, S., Heaton, H., Li, Q., McKenzie, D., Osher, S., and Yin, W. (2022). Jfb: Jacobian-free back-propagation for implicit networks. In *Proceedings of the AAAI Conference on Artificial Intelligence*, volume 36, pages 6648–6656.

Yin, W., McKenzie, D., and Wu Fung, S. (2022). Learning to optimize: Where deep learning meets optimization and inverse problems. *SIAM News*.

Zhang, J., Lei, Q., and Dhillon, I. (2018). Stabilizing gradients for deep neural networks via efficient svd parameterization. In *International Conference on Machine Learning*, pages 5806–5814. PMLR.

Zhao, Y., Zheng, S., and Yuan, X. (2023). Deep equilibrium models for snapshot compressive imaging. In *Proceedings of the AAAI Conference on Artificial Intelligence*, volume 37, pages 3642–3650.

A Generalization Bound for a Family of Implicit Networks: Supplementary Materials

A Proofs

For ease of presentation, we restate the results before their proofs.

A.1 Proof of Lemma 1

Lemma 1. *Under Assumption 4, the fixed point mapping $\Psi \times \mathcal{D} \rightarrow \mathbb{R}^n, (\psi, d) \mapsto x_{\psi, d}^*$ is Lipschitz with respect to θ with constant $L = \frac{L_\psi}{1 - L_x}$.*

Before beginning our proof, we note that since we treat the network parameters as inputs, we write $x_{\psi, d}^*$ as $x_d^*(\psi)$ in this proof for ease of presentation.

Proof. Fix an input $d \in \mathcal{D}$. For any $\psi_1, \psi_2 \in \Psi$, we have

$$\|x_d^*(\psi_1) - x_d^*(\psi_2)\| = \|T_{\psi_1}(x_d^*(\psi_1); d) - T_{\psi_2}(x_d^*(\psi_2); d)\| \quad (22)$$

$$= \|T_{\psi_1}(x_d^*(\psi_1); d) - T_{\psi_1}(x_d^*(\psi_2); d) + T_{\psi_1}(x_d^*(\psi_2); d) - T_{\psi_2}(x_d^*(\psi_2); d)\| \quad (23)$$

$$\leq \|T_{\psi_1}(x_d^*(\psi_1); d) - T_{\psi_1}(x_d^*(\psi_2); d)\| + \|T_{\psi_1}(x_d^*(\psi_2); d) - T_{\psi_2}(x_d^*(\psi_2); d)\| \quad (24)$$

$$\leq L_x \|x_d^*(\psi_2) - x_d^*(\psi_1)\| + L_\psi \|\psi_2 - \psi_1\|. \quad (25)$$

Since the first term in (25) contains $\|x_d^*(\psi_1) - x_d^*(\psi_2)\|_2$, we can expand this term again following the same procedure (22)–(25). Expanding N times, we obtain

$$\|x_d^*(\psi_1) - x_d^*(\psi_2)\| \leq L_x \|x_d^*(\psi_2) - x_d^*(\psi_1)\| + L_\psi \|\psi_2 - \psi_1\| \quad (26)$$

$$\leq L_x (L_x \|x_d^*(\psi_2) - x_d^*(\psi_1)\| + L_\psi \|\psi_2 - \psi_1\|) + L_\psi \|\psi_2 - \psi_1\| \quad (27)$$

$$\vdots \quad (28)$$

$$\leq (L_x)^{N+1} \|x_d^*(\psi_2) - x_d^*(\psi_1)\| + L_\psi \sum_{k=0}^N (L_x)^k \|\psi_2 - \psi_1\|. \quad (29)$$

Taking the limit as $N \rightarrow \infty$ and using geometric series (since $L_x < 1$), we obtain

$$\|x_d^*(\psi_1) - x_d^*(\psi_2)\| \leq \frac{L_\psi}{1 - L_x} \|\psi_2 - \psi_1\|, \quad (30)$$

where we observe that the second term in (29) goes to 0. \square

A.2 Proof of Lemma 2

Lemma 2 . *Under Assumption 4, the mapping $\Theta \times \mathcal{D} \rightarrow \mathbb{R}^n, ((\phi, \psi), d) \mapsto P_\phi(x_{\psi, d}^*)$ is Lipschitz with respect to $\theta = (\phi, \psi)$ with constant $\hat{L} = \sqrt{(L_{P,x}L)^2 + L_{P,\phi}^2}$.*

Proof. Fix an input $d \in \mathcal{D}$. For any $\theta_1, \theta_2 \in \Theta$, we have $\theta_i = (\phi_i, \psi_i)$ and get

$$\|P_{\phi_1}(x_{\psi_1, d}^*) - P_{\phi_2}(x_{\psi_2, d}^*)\| = \|P_{\phi_1}(x_{\psi_1, d}^*) - P_{\phi_1}(x_{\psi_2, d}^*) + P_{\phi_1}(x_{\psi_2, d}^*) - P_{\phi_2}(x_{\psi_2, d}^*)\| \quad (31)$$

$$\leq \|P_{\phi_1}(x_{\psi_1, d}^*) - P_{\phi_1}(x_{\psi_2, d}^*)\| + \|P_{\phi_1}(x_{\psi_2, d}^*) - P_{\phi_2}(x_{\psi_2, d}^*)\| \quad (32)$$

$$\stackrel{\text{using Assumption 4}}{\leq} L_{P,x} \|x_{\psi_1, d}^* - x_{\psi_2, d}^*\| + L_{P,\phi} \|\phi_1 - \phi_2\| \quad (33)$$

$$\stackrel{\text{using Lemma 1}}{\leq} L_{P,x} L \|\psi_1 - \psi_2\| + L_{P,\phi} \|\phi_1 - \phi_2\| \quad (34)$$

$$= (L_{P,x} L, L_{P,\phi}) \cdot (\|\psi_1 - \psi_2\|, \|\phi_1 - \phi_2\|) \quad (35)$$

$$\leq \sqrt{(L_{P,x} L)^2 + (L_{P,\phi})^2} \sqrt{\|\psi_1 - \psi_2\|^2 + \|\phi_1 - \phi_2\|^2} \quad (36)$$

$$= \sqrt{(L_{P,x} L)^2 + (L_{P,\phi})^2} \|\theta_1 - \theta_2\| \quad (37)$$

□

A.3 Proof of Lemma 3

Lemma 3. *Under Assumptions 2, 3, and 4, we have*

$$\mathcal{R}_S(\ell \circ \mathcal{H}) \leq \frac{8L_\ell}{N} \int_0^{\sqrt{N}C_{\text{out}}/2} \sqrt{\log \mathcal{N}(\mathcal{M}, \|\cdot\|, r)} \, dr. \quad (38)$$

where L_ℓ is the Lipschitz constant of ℓ .

Proof. This proof is structured as follows. **Step 1**, we show that the pseudometric defined in (7) associated with the Rademacher process is simply the l_2 norm of the difference of two random variables. **Step 2**, we bound the Rademacher complexity (Definition 3) by another Rademacher process that only depends on the hypothesis function. **Step 3**, we bound the radius of the Rademacher process. **Step 4**, we obtain a bound on the Rademacher complexity using a covering number argument by plugging results from Steps 1 and 2 into Dudley's inequality.

Step 1. We introduce a specific subgaussian process and a representation for its pseudometric. Let \mathcal{T} be an index set and $z : \mathcal{T} \rightarrow \mathbb{R}^N$ a function. Furthermore, let $\epsilon \in \mathbb{R}^N$ be a Rademacher vector, i.e., a random vector with entries ± 1 . Then, the stochastic process $(Z_t)_{t \in \mathcal{T}}$ given by

$$Z_t := \sum_{i=1}^N \epsilon_i (z(t))_i = \epsilon^\top z(t), \quad (39)$$

is a Rademacher process, cf. (Foucart and Rauhut, 2013, p. 225). Moreover, this process is subgaussian and we get

$$\mathbb{E}|Z_s - Z_t|^2 = \mathbb{E}|\epsilon^\top (z(s) - z(t))|^2 = \|z(s) - z(t)\|^2. \quad (40)$$

Thus, we have that

$$d(Z_s, Z_t) = (\mathbb{E}|Z_s - Z_t|^2)^{1/2} = \|z(s) - z(t)\|. \quad (41)$$

Step 2. From Definition 3 and (12), we have that

$$R_S(\ell \circ \mathcal{H}) = \mathbb{E}_\epsilon \sup_{h \in \mathcal{H}} \frac{1}{N} \sum_{i=1}^N \epsilon_i \ell(h(d_i), y_i) \quad (42)$$

with $\epsilon \in \mathbb{R}^N$ a Rademacher vector.

Now, we need the so-called vector-valued contraction lemma Maurer (2016). To point out that it is applicable in our case, we cite it here in full, just slightly adjusting it to our notation:

Contraction lemma (Maurer, 2016, Corollary 4) Let \mathcal{X} be any set, $(x_1, \dots, x_n) \in \mathcal{X}^n$, let F be a class of functions $f : \mathcal{X} \rightarrow \ell_2$ and let $h_i : \ell_2 \rightarrow \mathbb{R}$ be Lipschitz continuous functions with constant L . Here, ℓ_2 denotes the space of square summable sequences. Then,

$$\mathbb{E}_\epsilon \sup_{f \in F} \sum_i \epsilon_i h_i(f(x_i)) \leq \sqrt{2} L \mathbb{E}_\epsilon \sup_{f \in F} \sum_{i,k} \tilde{\epsilon}_{ik} (f(x_i))_k,$$

where $\epsilon \in \mathbb{R}^n$ is a Rademacher vector, $\tilde{\epsilon}_{ik}$ is an independent doubly indexed Rademacher sequence and $(f(x_i))_k$ is the k -th component of $f(x_i)$.

Since ℓ is Lipschitz by Assumption 2, we have that by the contraction lemma, choosing h_i in the contraction lemma as $l(\cdot, y_i)$ and embedding \mathbb{R}^m in ℓ_2 ,

$$\mathbb{E}_\epsilon \sup_{h \in \mathcal{H}} \sum_{i=1}^N \epsilon_i \ell(h(d_i), y_i) \leq \sqrt{2} L_\ell \mathbb{E}_\epsilon \sup_{h \in \mathcal{H}} \sum_{i=1}^N \sum_{j=1}^m \tilde{\epsilon}_{ij} (h(d_i))_j, \quad (43)$$

where $\tilde{\epsilon} \in \mathbb{R}^{N \times m}$ is a Rademacher matrix and L_ℓ is the Lipschitz constant of ℓ . Thus, we can bound the Rademacher complexity by plugging (43) into (42) to get

$$R_S(\ell \circ \mathcal{H}) \leq \frac{\sqrt{2}L_\ell}{N} \mathbb{E}_{\tilde{\epsilon}} \sup_{h \in \mathcal{H}} \sum_{i=1}^N \sum_{j=1}^m \tilde{\epsilon}_{ij} (h(d_i))_j = \frac{\sqrt{2}L_\ell}{N} \mathbb{E}_{\tilde{\epsilon}} \sup_{M \in \mathcal{M}} \sum_{i=1}^N \sum_{j=1}^m \tilde{\epsilon}_{ij} M_{ij} \quad (44)$$

where \mathcal{M} is defined in (4).

Step 3. Next, using **Step 1**, we note that the process $(Z_M)_{M \in \mathcal{M}}$ given by

$$Z_M = \sum_{i=1}^N \sum_{j=1}^m \tilde{\epsilon}_{ij} M_{ij}, \quad (45)$$

i.e., the double sum from the right-hand-side of (44), is a Rademacher process. Thus, from (9), and noting the identity

$$\begin{aligned} \mathbb{E}_{\tilde{\epsilon}} \left| \sum_{i=1}^N \sum_{j=1}^m \tilde{\epsilon}_{ij} M_{ij} \right|^2 &= \mathbb{E}_{\tilde{\epsilon}} \left(\sum_{i=1}^N \sum_{j=1}^m \tilde{\epsilon}_{ij} M_{ij} \right)^2 \\ &= \mathbb{E}_{\tilde{\epsilon}} \left(\sum_{i=1}^N \sum_{j=1}^m \tilde{\epsilon}_{ij}^2 M_{ij}^2 + \sum_{i=1}^N \sum_{j=1}^m \sum_{\substack{k=1 \\ k \neq i}}^N \sum_{\substack{l=1 \\ l \neq j}}^m \tilde{\epsilon}_{ij} M_{ij} \tilde{\epsilon}_{kl} M_{kl} \right) \\ &= \sum_{i=1}^N \sum_{j=1}^m M_{ij}^2 + \sum_{i=1}^N \sum_{j=1}^m \sum_{\substack{k=1 \\ k \neq i}}^N \sum_{\substack{l=1 \\ l \neq j}}^m \underbrace{\mathbb{E}_{\tilde{\epsilon}} \tilde{\epsilon}_{ij} M_{ij} \tilde{\epsilon}_{kl} M_{kl}}_{=0}, \end{aligned} \quad (46)$$

we estimate the radius of this process as

$$\Delta(\mathcal{M}) = \sup_{M \in \mathcal{M}} \sqrt{\mathbb{E}_{\tilde{\epsilon}} |Z_M|^2} \quad (47)$$

$$= \sup_{M \in \mathcal{M}} \sqrt{\mathbb{E}_{\tilde{\epsilon}} \left| \sum_{i=1}^N \sum_{j=1}^m \tilde{\epsilon}_{ij} M_{ij} \right|^2} \quad (48)$$

$$= \sup_{M \in \mathcal{M}} \sqrt{\sum_{i=1}^N \sum_{j=1}^m |M_{ij}|^2} \quad (49)$$

$$= \sup_{h \in \mathcal{H}} \sqrt{\sum_{i=1}^N \|h(d_i)\|^2} \quad (50)$$

$$= \sup_{\theta=(\phi,\psi) \in \Theta} \sqrt{\sum_{i=1}^N \|P_\psi(x_{\psi,d_i}^*)\|^2} \quad (51)$$

$$\leq \sqrt{NC_{\text{out}}}, \quad (52)$$

where the last inequality is a result of Assumption 3.

Step 4. Starting with (44) and then applying Dudley's inequality (see Theorem 1) on the right hand side and plugging in the radius bound from (52) into , we arrive at our result

$$R_S(\ell \circ \mathcal{H}) \leq \frac{\sqrt{2}L_\ell}{N} \mathbb{E}_{\tilde{\epsilon}} \sup_{M \in \mathcal{M}} \sum_{i=1}^N \sum_{j=1}^m \tilde{\epsilon}_{ij} M_{ij} \quad (53)$$

$$\leq \frac{8L_\ell}{N} \int_0^{\frac{\sqrt{NC_{\text{out}}}}{2}} \sqrt{\log(\mathcal{N}(\mathcal{M}, \|\cdot\|, r))} dr \quad (54)$$

where \mathcal{N} is the covering number defined in Definition 2, and the pseudometric function $\|\cdot\|$ is given by (41) from Step 1. \square

A.4 Proof of Lemma 4

Lemma 4. *Under Assumptions 4 and 3,*

$$\mathcal{N}(\mathcal{M}, \|\cdot\|, r) \leq \left(1 + \frac{2\hat{L}C_{\text{params}}}{r}\right)^p, \quad (55)$$

where $C_{\text{params}} = \sqrt{C_{\text{params},\Phi}^2 + C_{\text{params},\Psi}^2}$.

Proof. Let $r > 0$ and $L = \frac{L_\psi}{1 - L_x}$ from Lemma 1 and $\hat{L} = \sqrt{((L_{P,x}L)^2 + L_{P,\phi}^2)}$ from Lemma 2. Moreover, let $k := \mathcal{N}(\Theta, \|\cdot\|, \frac{r}{\hat{L}})$. Then, there are $\theta_1, \dots, \theta_k \in \Theta$ with $\theta_i = (\phi_i, \psi_i)$ such that

$$\Theta \subset \bigcup_{i=1}^k B_{\frac{r}{\hat{L}}}(\theta_i). \quad (56)$$

Here, $B_r(x)$ denotes a ball with radius $r > 0$ centered at x , i.e., $B_r(x) := \{y \in X : \|x - y\|_X < r\}$ for any normed vector space $(X, \|\cdot\|_X)$. Let $y \in \mathcal{M}$. By definition of \mathcal{M} (cf. (4)), there is a $\theta = (\phi, \psi) \in \Theta$ such that $y = P_\phi(x_{\psi,d}^*)$. By (56), there is $j \in \{1, \dots, k\}$ such that $\theta \in B_{\frac{r}{\hat{L}}}(\theta_j)$. With this we get

$$\|y - P_{\phi_j}(x_{\psi_j,D}^*)\| = \|P_\phi(x_{\psi,d}^*) - P_{\phi_j}(x_{\psi_j,D}^*)\| \leq \hat{L}\|\theta - \theta_j\| \leq \hat{L}\frac{r}{\hat{L}} = r. \quad (57)$$

Thus, we have shown $y \in B_r(P_{\phi_j}(x_{\psi_j,D}^*))$. Since $x \in \mathcal{M}$ was arbitrary, we get

$$\mathcal{M} \subset \bigcup_{i=1}^k B_r(P_{\phi_i}(x_{\psi_j,D}^*)). \quad (58)$$

This immediately implies

$$\mathcal{N}(\mathcal{M}, \|\cdot\|, r) \leq k = \mathcal{N}(\Theta, \|\cdot\|, \frac{r}{\hat{L}}). \quad (59)$$

By Assumption 3, we have, for $\theta = (\phi, \psi) \in \Theta$, that $\|\theta\| \leq \sqrt{\|\phi\|^2 + \|\psi\|^2} \leq \sqrt{C_{\text{params},\Phi}^2 + C_{\text{params},\Psi}^2} =: C_{\text{params}}$ and thus

$$\Theta = \{\theta \in \mathbb{R}^p : \|\theta\| \leq C_{\text{params}}\} = \{\theta \in \mathbb{R}^p : \frac{1}{C_{\text{params}}}\|\theta\| \leq 1\} \quad (60)$$

Thus, Θ is (contained in) the closed one ball of \mathbb{R}^p with respect to the norm $\frac{1}{C_{\text{params}}}\|\cdot\|$. Using (Foucart and Rauhut, 2013, Proposition C.3), we get for any $t > 0$

$$\mathcal{N}\left(\Theta, \frac{1}{C_{\text{params}}}\|\cdot\|, t\right) \leq \left(1 + \frac{2}{t}\right)^p. \quad (61)$$

Noting that $\|\cdot\| < t$ is equivalent to $c\|\cdot\| < ct$ for any $c > 0$, it holds that

$$\mathcal{N}(\Theta, \|\cdot\|, t) = \mathcal{N}(\Theta, c\|\cdot\|, ct). \quad (62)$$

Combining the arguments collected above results in

$$\begin{aligned} \mathcal{N}(\Theta, \|\cdot\|, \frac{r}{\hat{L}}) &\stackrel{(62)}{=} \mathcal{N}\left(\Theta, \frac{1}{C_{\text{params}}}\|\cdot\|, \frac{1}{C_{\text{params}}}\frac{r}{\hat{L}}\right) \\ &\stackrel{(61)}{\leq} \left(1 + \frac{2}{\frac{1}{C_{\text{params}}}\frac{r}{\hat{L}}}\right)^p = \left(1 + \frac{2\hat{L}C_{\text{params}}}{r}\right)^p, \end{aligned} \quad (63)$$

which, together with (59), concludes the proof. \square

A.5 Proof of Lemma 5

Lemma 5. *Under Assumptions 1, 2, there exists a constant $C_\ell > 0$ such that*

$$|\ell(P_\phi(x_{\psi,d}^*, y))| \leq C_\ell \quad \forall (d, y) \sim \mathbb{P}_{true}, \forall \theta = (\phi, \psi) \in \Theta. \quad (64)$$

Proof. Since \mathcal{D} is a compact set (Assumption 1) and ℓ is continuous with respect to its arguments (Assumption 2), we have that ℓ must be bounded. \square

A.6 Proof of Theorem 3

Theorem 3. *Under Assumptions 1–4, for any $\theta \in \Theta$ and $\delta \in (0, 1)$, we have*

$$\begin{aligned} \mathcal{L}(\theta) &\leq \hat{\mathcal{L}}(\theta) \\ &+ 8L_\ell C_{\text{out}} \sqrt{\frac{p}{N} \cdot \log \left(e \cdot \left(1 + \frac{4\hat{L}C_{\text{params}}}{\sqrt{NC_{\text{out}}}} \right) \right)} \\ &+ 4C_\ell \sqrt{\frac{2\log(4/\delta)}{N}} \end{aligned} \quad (65)$$

with probability $1 - \delta$.

Proof. Plugging the result from Lemma 4 into Lemma 3, we have that

$$R_S(\ell \circ \mathcal{H}) \leq \frac{8L_\ell}{N} \int_0^{\sqrt{NC_{\text{out}}}/2} \sqrt{\log \left(1 + \frac{2\hat{L}C_{\text{params}}}{r} \right)^p} dr \quad (66)$$

$$= \frac{8L_\ell \sqrt{p}}{N} \int_0^{\sqrt{NC_{\text{out}}}/2} \sqrt{\log \left(1 + \frac{2\hat{L}C_{\text{params}}}{r} \right)} dr. \quad (67)$$

Using

$$\int_0^\alpha \sqrt{1 + \frac{\beta}{t}} dt \stackrel{\varphi(t) = \frac{\beta}{t}}{=} \int_0^\alpha \sqrt{1 + \frac{1}{\varphi(t)}} \beta \varphi'(t) dt = \beta \int_0^{\frac{\alpha}{\beta}} \sqrt{1 + \frac{1}{t}} dt, \quad (68)$$

and (Foucart and Rauhut, 2013, Lemma C.9), we get that

$$\int_0^\alpha \sqrt{1 + \frac{\beta}{t}} dt \leq \alpha \sqrt{\log \left(e \cdot \left(1 + \frac{\beta}{\alpha} \right) \right)}, \quad \text{for all } \alpha, \beta > 0. \quad (69)$$

Consequently, by setting $\beta = 2\hat{L}C_{\text{params}}$ and $\alpha = \frac{\sqrt{NC_{\text{out}}}}{2}$, we can further bound (67) as

$$R_S(\ell \circ \mathcal{H}) \leq \frac{8L_\ell \sqrt{p}}{N} \frac{\sqrt{NC_{\text{out}}}}{2} \sqrt{\log \left(e \cdot \left(1 + \frac{2\hat{L}C_{\text{params}}}{\sqrt{NC_{\text{out}}}/2} \right) \right)} \quad (70)$$

$$= \frac{4L_\ell C_{\text{out}} \sqrt{p}}{\sqrt{N}} \sqrt{\log \left(e \cdot \left(1 + \frac{4\hat{L}C_{\text{params}}}{\sqrt{NC_{\text{out}}}} \right) \right)}. \quad (71)$$

Plugging this bound into Theorem 2, we obtain our desired result. \square

A.7 Proof of Lemma 6

Lemma 6. *Let T_ψ be given by (18). Under Assumption 3, T_ψ satisfies Assumption 4 with $L_x = \|W\|$ and $L_\psi = \sqrt{C_{\text{out}}^2 + C_d^2 + 1}$.*

Proof. Since $\|W\| < 1$ and σ is 1-Lipschitz, we have contractivity guaranteed Ryu and Yin (2022). Thus, we only need to show Lipschitzness in ψ on the set of fixed points. Let $\psi_1 = (W_1, U_1, b_1) \in \Psi$ and $\psi_2 = (W_2, U_2, b_2) \in \Psi$ and $d \in \mathcal{D}$. Moreover, let $x \in \mathcal{X}^* = \{x \in \mathbb{R}^n : \exists \psi \in \Psi, d \in \mathcal{D} \text{ s.t. } x = T_\psi(x; d)\}$. We have

$$\|T_{\psi_1}(x; d) - T_{\psi_2}(x; d)\| = \|\sigma(W_1 x + U_1 d + b_1) - \sigma(W_2 x + U_2 d + b_2)\| \quad (72)$$

$$\leq \|(W_1 x + U_1 d + b_1) - (W_2 x + U_2 d + b_2)\| \quad (73)$$

$$\leq \|(W_1 - W_2)x\| + \|(U_1 - U_2)d\| + \|b_1 - b_2\| \quad (74)$$

$$\stackrel{\text{using } x \in \mathcal{X}^* \text{ and Assumption 3}}{\leq} C_{\text{out}}\|W_1 - W_2\| + C_d\|U_1 - U_2\| + \|b_1 - b_2\| \quad (75)$$

$$= (C_{\text{out}}, C_d, 1) \cdot (\|W_1 - W_2\|, \|U_1 - U_2\|, \|b_1 - b_2\|) \quad (76)$$

$$\leq \sqrt{C_{\text{out}}^2 + C_d^2 + 1} \sqrt{\|W_1 - W_2\|^2 + \|U_1 - U_2\|^2 + \|b_1 - b_2\|^2} \quad (77)$$

$$= L_\psi \|\psi_1 - \psi_2\| \quad (78)$$

where $L_\psi := \sqrt{C_{\text{out}}^2 + C_d^2 + 1}$ and we have used the Cauchy-Schwarz inequality and that $\|\cdot\|$ is the Euclidean norm. \square

A.8 Proof of Lemma 7

Lemma 7. Let T_ψ be given by (19). Under Assumption 3, T_ψ satisfies Assumption 4 with $L_\psi = \alpha \sqrt{4(C_{\text{params}}^2 + 1)C_{\text{out}}^2 + C_d^2 + 1}$ and $L_x < 1$.

Proof. It is well-known that T is contractive in x Ryu and Yin (2022); Winston and Kolter (2020). Thus, we only need to show Lipschitzness in ψ on the set of fixed points.

For $i = 1, 2$, let $\psi_i = (A_i, B_i, U_i, b_i)$ and $W_i = (1 - m)I - A_i^\top A_i + B_i - B_i^\top$. Moreover, let $F_W = I - \alpha(I - W)$ and $x \in \mathcal{X}^* = \{x \in \mathbb{R}^n : \exists \psi \in \Psi, d \in \mathcal{D} \text{ s.t. } x = T_\psi(x; d)\}$. Then,

$$\|T_{\psi_1}(x; d) - T_{\psi_2}(x; d)\| = \|\sigma(F_{W_1}x + \alpha(U_1 d + b_1)) - \sigma(F_{W_2}x + \alpha(U_2 d + b_2))\| \quad (79)$$

$$\leq \|(F_{W_1}x + \alpha(U_1 d + b_1)) - (F_{W_2}x + \alpha(U_2 d + b_2))\| \quad (80)$$

$$\leq \|(I - \alpha(I - W_1))x - (I - \alpha(I - W_2))x\| + \|\alpha(U_1 d + b_1) - \alpha(U_2 d + b_2)\| \quad (81)$$

$$= \|\alpha(W_1 - W_2)x\| + \alpha\|(U_1 - U_2)d + b_1 - b_2\| \quad (82)$$

$$\leq \alpha(\|W_1 - W_2\|\|x\| + \|U_1 - U_2\|\|d\| + \|b_1 - b_2\|) \quad (83)$$

$$\leq \alpha(C_{\text{out}}\|W_1 - W_2\| + C_d\|U_1 - U_2\| + \|b_1 - b_2\|) \quad (84)$$

where the second inequality is due to 1-Lipschitzness of σ and the last inequality arises from Assumption 3 and $x \in \mathcal{X}^*$ to get $\|x\| \leq C_{\text{out}}$ and Assumption 1 to get $\|d\| \leq C_d$, where $C_d = \max_d \{ \|d\| : d \in \mathcal{D} \}$.

Recalling $W_i = (1 - m)I - A_i^\top A_i + B_i - B_i^\top$, we get

$$\|W_2 - W_1\| = \|(1 - m)I - A_1^\top A_1 + B_1 - B_1^\top - ((1 - m)I - A_2^\top A_2 + B_2 - B_2^\top)\| \quad (85)$$

$$= \|A_2^\top A_2 - A_1^\top A_1 + B_1 - B_1^\top - B_2 + B_2^\top\| \quad (86)$$

$$\leq \|A_2^\top (A_2 - A_1) + (A_2^\top - A_1^\top)A_1\| + \|B_1 - B_2 + B_2^\top - B_1^\top\| \quad (87)$$

$$\leq \|A_2^\top (A_2 - A_1)\| + \|(A_2^\top - A_1^\top)A_1\| + \|B_1 - B_2\| + \|B_2^\top - B_1^\top\| \quad (88)$$

$$\stackrel{\text{Assumption 3}}{\leq} 2C_{\text{params}}\|A_2 - A_1\| + 2\|B_2 - B_1\|. \quad (89)$$

Combined with the above, we get

$$\|T_{\psi_1}(x; d) - T_{\psi_2}(x; d)\| \quad (90)$$

$$\leq \alpha(C_{\text{out}}(2C_{\text{params}}\|A_2 - A_1\| + 2\|B_2 - B_1\|) + C_d\|U_1 - U_2\| + \|b_1 - b_2\|) \quad (91)$$

$$= \alpha(2C_{\text{params}}C_{\text{out}}, 2C_{\text{out}}, C_d, 1) \cdot (\|A_2 - A_1\|, \|B_2 - B_1\|, \|U_1 - U_2\|, \|b_1 - b_2\|) \quad (92)$$

$$\leq \alpha \sqrt{4C_{\text{params}}^2 C_{\text{out}}^2 + 4C_{\text{out}}^2 + C_d^2 + 1} \sqrt{\|A_2 - A_1\|^2 + \|B_2 - B_1\|^2 + \|U_1 - U_2\|^2 + \|b_1 - b_2\|^2} \quad (93)$$

$$= \alpha \sqrt{4(C_{\text{params}}^2 + 1)C_{\text{out}}^2 + C_d^2 + 1} \|\psi_1 - \psi_2\|, \quad (94)$$

where we have used the Cauchy-Schwarz inequality and that $\|\cdot\|$ is the Euclidean norm. Thus, we have that the Lipschitz constant of T w.r.t $\psi = (A, B, U, b)$ is given by

$$L_\psi = \alpha \sqrt{4(C_{\text{params}}^2 + 1)C_{\text{out}}^2 + C_d^2 + 1}. \quad (95)$$

This shows that that Assumption 4 is satisfied for this architecture. \square

A.9 Proof of Lemma 8

Lemma 8. *Let T_ψ be given by (21). Under Assumption 3, T_ψ satisfies Assumption 4 with $L_\psi = 2\alpha C_{\text{out}} C_{\text{params}, \Psi}$ and $L_x < 1$.*

Proof. Contractivity of T in x is well-known when α is prescribed as above Ryu and Yin (2022). Thus, we only need to show Lipschitzness of T with respect to R at the fixed points.

Let $R_1, R_2 \in \mathbb{R}^{n_1 \times n}$ be given. Let $x \in \mathcal{X}^* = \{x \in \mathbb{R}^n : \exists \psi \in \Psi, d \in \mathcal{D} \text{ s.t. } x = T_\psi(x; d)\}$ belong to the set of fixed points. We have

$$\|T_{R_1}(x; d) - T_{R_2}(x; d)\| \quad (96)$$

$$= \|x - \alpha(A^\top(Ax - d) + R_1^\top R_1 x) - (x - \alpha(A^\top(Ax - d) + R_2^\top R_2 x))\| \quad (97)$$

$$= \|\alpha(R_2^\top R_2 - R_1^\top R_1)x\| \quad (98)$$

$$\stackrel{\text{using } x \in \mathcal{X}^* \text{ and Assumption 3}}{\leq} \alpha C_{\text{out}} \|R_2^\top R_2 - R_2^\top R_1 + R_2^\top R_1 - R_1^\top R_1\| \quad (99)$$

$$\leq \alpha C_{\text{out}} (\|R_2^\top R_2 - R_2^\top R_1\| + \|R_2^\top R_1 - R_1^\top R_1\|) \quad (100)$$

$$\stackrel{\text{using Assumption 3}}{\leq} 2\alpha C_{\text{out}} C_{\text{params}, \Psi} \|R_2 - R_1\| \quad (101)$$

\square

A.10 Lipschitzness of Cross Entropy of Softmax

Lemma 9. *Let $s(x) = \frac{\exp(x)}{\sum_{i=1}^n \exp(x_i)}$ be the softmax function, and let $y \in \mathbb{R}^n$ be a one-hot vector. Moreover, consider function $g : \mathbb{R}^n \rightarrow \mathbb{R}, x \mapsto C(s(x), y)$, where C is the cross entropy function. Then, then g is well-defined and Lipschitz with constant 2.*

Proof. Suppose y has value 1 in the k^{th} entry. Let $x \in \mathbb{R}^n$. Then, since the exponential function is never zero, we have

$$s(x)_j = \frac{\exp(x_j)}{\sum_{i=1}^n \exp(x_i)} > 0, \quad j = 1, \dots, n. \quad (102)$$

Thus,

$$g(x) = -y^\top \log(s(x)) \quad (103)$$

$$= -\log(s(x)_k) \quad (104)$$

is well-defined.

Next, we derive a formula for the gradient of g . We have

$$\partial_{x_j} g(x) = -\frac{1}{s(x)_k} \partial_{x_j} (s(x)_k) = \begin{cases} \frac{\exp(x_j)}{\sum_{i=1}^n \exp(x_i)} & \text{when } j \neq k \\ \frac{\exp(x_k)}{\sum_{i=1}^n \exp(x_i)} - 1 & \text{when } j = k. \end{cases} \quad (105)$$

Thus, the gradient is given by $\nabla g(x) = s(x) - y$. Taking its norm, we estimate the Lipschitz constant of g to be

$$\|\nabla g(x)\|_2 = \|s(x) - y\|_2 \leq \underbrace{\|s(x)\|_2}_{\leq \|s(x)\|_1 = 1} + \|y\|_2 \quad (106)$$

$$\leq 2. \quad (107)$$

where we note $\|y\|_2 = 1$ for one-hot vectors. \square

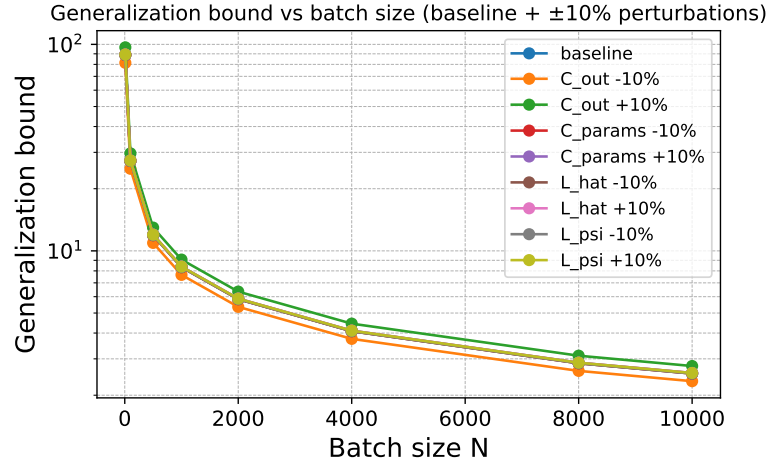


Figure 3: Illustration of robustness of generalization bound under $\pm 10\%$ perturbations to L_ψ , \hat{L} , C_{out} , and C_{params} .

B Robustness Experiment

We show that the derived generalization bound is robust to perturbations to the parameters. In particular, we consider $\pm 10\%$ perturbations to the parameters C_{params} , C_{out} , L_ψ , and \hat{L} using the Contractive Single Layer architecture on the MNIST dataset. We note that one can only see three out of the nine bounds due to the similarity to one another.